Published in final edited form as:

Neuroendocrinology. 2017 ; 104(2): 194–208. doi:10.1159/000446114.

Chronic unpredictable mild stress induces loss of GABA inhibition in corticotrophin-releasing hormone-expressing neurons through NKCC1 upregulation

Yonggang Gao[#1], **Jing-Jing Zhou**[#1], **Yun Zhu**[1,2], **Therese Kosten**[3], and **De-Pei Li**[4]

[1] Department of Anesthesiology & Perioperative Medicine, The University of Texas MD Anderson Cancer Center

[3] Department of Psychology, the University of Houston

[4] Department of Critical Care, The University of Texas MD Anderson Cancer Center

[#] These authors contributed equally to this work.

Abstract

Introduction—Prolonged and repeated stresses cause hyperactivity of the hypothalamic-pituitary-adrenal (HPA) axis. The corticotrophin-releasing hormone (CRH)-expressing neurons in the hypothalamic paraventricular nucleus (PVN) are an essential component of the HPA axis.

Materials and Methods—Chronic unpredictable mild stress (CUMS) were performed in Sprague-Dawley rats. GABA reversal potential (E_{GABA}) were determined by using gramicidin-perforated recordings in identified PVN-CRH neurons through expressing enhanced green fluorescent protein (eGFP) driven by CRH promoter. Plasma corticosterone (CORT) levels were measured in rats implanted with cannula targeting lateral ventricles and the PVN.

Results—Blocking the $GABA_A$ receptor in the PVN with gabazine significantly increased Plasma CORT levels in unstressed rats but did not change CORT levels in CUMS rats. CUMS caused a depolarizing shift in E_{GABA} in PVN-CRH neurons compared with E_{GABA} in PVN-CRH neurons in unstressed rats. Furthermore, CUMS induced a long-lasting increase in expression levels of cation chloride co-transporter Na^+-K^+-Cl^--Cl^- (NKCC1) in the PVN, but a transient decrease in expression levels of K^+-Cl^--Cl^- (KCC2) in the PVN, which returned to the basal level 5 days after CUMS treatment. The NKCC1 inhibitor bumetanide decreased the basal firing activity of PVN-CRH neurons and normalized E_{GABA} and the gabazine-induced excitatory effect on PVN-CRH neurons in CUMS rats. In addition, central administration of bumetanide decreased basal circulating CORT levels in CUMS rats.

Corresponding Author De-Pei Li, Department of Critical Care, The University of Texas MD Anderson Cancer Center, 1515 Holcombe Boulevard, Houston, TX 77030, USA. Tel: (713) 563-4887; Fax: (713) 794-4590; dpli@mdanderson.org.
[2]Present affiliation: Department of Otorhinolaryngology, Union Hospital of Tongji Medical College, Huazhong University of Science and Technology, Wuhan, Hubei 430022, China

Author Contributions:

D-P. L. and T. K. designed the study. Y. G., J-J. Z., Y. Z., and D-P. L. performed the experiments and analyzed the data. Y. G, J-J. Z, and D-P. L wrote the manuscript. T. K. revised and commented on the manuscript.

Competing financial interests

The authors declare no competing financial interests.

Conclusions—These data suggest that chronic stress impairs GABAergic inhibition, resulting in HPA axis hyperactivity through upregulation of NKCC1.

Keywords

hypothalamus; chronic stress; GABA inhibitory neurotransmission; cation Cl^- co-transporters

Introduction

The physiological stress response is pivotal for maintaining homeostasis and survival. However, prolonged and repeated exposure to stressors can cause psychopathological disorders such as depression. Chronic stress is a critical environmental risk factor for depression, the etiology of which involves hyperactivity of the hypothalamic-pituitary-adrenal (HPA) axis [1-3]. However, the mechanisms underlying the hyperactivity of the HPA axis in chronic stress remain unknown. Corticotrophin-releasing hormone (CRH)-expressing neurons in the hypothalamic paraventricular nucleus (PVN) (PVN-CRH neurons) are an essential component of the HPA axis and critically regulate HPA axis activity and stress responses [3]. Despite the critical role of PVN-CRH neurons in the regulation of HPA axis activity, it has been difficult to functionally unravel the cellular mechanisms that regulate PVN-CRH neurons because they cannot be distinguished morphologically from other types of neurons. Visualizing CRH-expressing neurons through immunohistochemical analysis is difficult without prior administration of compounds that inhibit axonal transport to promote the somatic accumulation of neuropeptides [4]. In transgenic mice, PVN-CRH neurons can be tagged by specifically expressing green fluorescent protein driven by the endogenous Crh promoter [5-7]. However, many studies use established rat stress models to study HPA axis activity. Thus, we developed a novel genetic approach to reliably identify PVN-CRH neurons by expressing enhanced green fluorescent protein (eGFP) under the control of rat Crh promoter. This allowed us to determine the alteration of biochemical and electrophysiological properties in eGFP-tagged CRH-expressing neurons in response to chronic stress.

CRH-expressing neurons receive both inhibitory GABAergic and excitatory noradrenergic and glutamatergic inputs [8-11]. GABAergic synaptic inputs importantly regulate PVN-CRH neuron activity [12]. $GABA_A$ receptors are ligand-gated ion channels with a predominant permeability to Cl^- [13, 14]. The GABA reversal potential (E_{GABA}) is a key determinant of the neuronal response to activation of $GABA_A$ receptors. When E_{GABA} is lower than the cell resting membrane potential, $GABA_A$ receptor activation elicits a hyperpolarization of the cell membrane [15, 16]; however, when E_{GABA} is higher than (as a result of high intracellular Cl^- concentration), $GABA_A$ receptor activation results in depolarization of the cell membrane and enhanced neuronal excitability. The cation-chloride co-transporters, including Na^+-K^+-Cl^--Cl^- (NKCC1) and K^+-Cl^--Cl^- (KCC2), play important roles in determining E_{GABA} through regulation of the intracellular Cl^- concentration [17, 18].

It has been shown that E_{GABA} is altered in several types of stress, including acute stress [19, 20], chronic hyperosmotic stress [21], and early life stress [22], and in some neuronal disorders, including status epilepticus [23], injury [24], neuropathic pain [25-27], cellular

oxidative stress [28], trauma [24, 29], seizure [30-32], and hypertension [33, 34]. However, the mechanism of GABA response in CUMS is not fully understood. It has been shown that both acute stress and chronic stress reduce GABA release in the PVN [35, 36]. Downregulation of KCC2 is responsible for the depolarizing shift of E_{GABA} in various types of neurons in acute stress [19, 20], status epilepticus [23], injury [24], neuropathic pain [25-27], cellular oxidative stress [28], trauma [24, 29], and seizure [30-32]. In contrast, upregulation of NKCC1 was shown to be responsible for the depolarizing shift of E_{GABA} in chronic hyperosmotic stress [21] and early life stress [22]. However, the aforementioned studies provide little information about the dynamic changes of NKCC1 and KCC2 in the post-stress period. In this study, we tested the hypothesis that a depolarizing shift in E_{GABA} induced by upregulation of NKCC1 in PVN-CRH neurons contributes to the hyperactivity of the HPA axis in chronic stress. In addition, we determined the dynamic changes of these cationchloride cotransporters in response to chronic stress.

Materials and methods

Animals

This study was carried out by using male Sprague-Dawley rats (8-12 weeks old, Harlan, Indianapolis, IN). The rats were housed in standard conditions (22-24°C) with a 12-h light/dark cycle. The experimental protocols and surgical procedures were approved by the Animal Care and Use Committee of The University of Texas MD Anderson Cancer Center and conformed to the National Institutes of Health guidelines on the ethical use of animals.

Chronic unpredictable mild stress (CUMS) rat model

The CUMS rat model provides a good analogy to the precipitation of depression by chronic, low-grade stressors in humans [37, 38]. The CUMS model was developed according to an established paradigm: male Sprague-Dawley rats were exposed to 2 stressors per day from a total of 8 stressors (cage rotation, cold isolation, light off, light on, forced swim, restraint stress, isolation housing, and food/water deprivation) for 11 days; stressors were randomly varied from day to day [39-41]. To avoid the influence of the final stressor in the CUMS paradigm, all measurements, including measurement of circulating corticosterone (CORT), sucrose preference test, and electrophysiological recordings, were performed 5-10 days after the CUMS treatment was finished.

We measured serum CORT levels and performed a sucrose preference test [37, 38] to validate that the CUMS procedure was stressful. The serum was isolated from blood collected from the orbital sinus by high-speed centrifugation in serum collection tubes (14,000 rpm, 5 min). CORT concentrations were measured by using an enzyme immunoassay and compared with a standard curve of known CORT concentration per the manufacturer's instructions (Enzo Life Sciences) [20]. To minimize variability, all samples from each experiment were stored at −80°C before testing in parallel. In addition, to determine whether prolonged CUMS treatment induces higher circulating CORT levels than does the 11-day CUMS treatment, another group of rats were exposed to CUMS for 20 days.

For the sucrose preference test, the rats were first trained to drink 0.7% sucrose solution for 48 h. Then, each rat was simultaneously exposed to 1 bottle containing 0.7% sucrose solution and 1 bottle containing tap water. The 2 bottles were randomly positioned (right/left) and positioning was counterbalanced across the rats. Because sucrose preference differs between the dark and light phases [42, 43], we performed sucrose preference tests in both light on (1000–1100 h) and off (1800–1900 h) phases. The intake volumes of tap water or sucrose solution were determined in unstressed and CUMS groups by weighing the bottles. We summarized the intake volumes of tap water or sucrose solution in both light on and light off phases. The preference for sucrose was calculated as a percentage of consumed sucrose solution of the total amount of liquid intake. Sucrose preference was calculated as the divided by total fluid intake (water intake + sucrose intake) × 100.

Identification of PVN-CRH neurons

To efficiently identify CRH-expressing neurons in rat PVN, we constructed a viral plasmid containing rat Crh promoter [44] and eGFP and integrated this plasmid into an adeno-associated virus (AAV) vector construct. The full-length promoter fragment (−2125/+94) was subcloned into the AAV vector expression cassette by using short regulatory elements (woodchuck post regulatory element 2 [WPRE2] and short synthetic polyadenylation [SpA]). The serotype of the AAV used was chimeric AAV1/2, which had AAV1 and AAV2 capsid proteins in a 1:1 ratio. The chimeric AAV1/2 serotype has been widely used [45]. The packaging was performed by Genedetect, Ltd (Auckland, New Zealand). The viral vector construct contained the following components: inverted terminal repeat sequence from AAV2, rat Crh promoter, eGFP, WPRE2, and SpA. The titers of the packaged AAV-Crh promoter eGFP were 1×10^{13} GC/ml. This viral construct was delivered into the rat PVN in vivo through microinjection (100 nl) (stereotaxic coordinates: 1.8-2.1 mm caudal from the bregma, 0.5 mm lateral to the midline, and 7.3-7.6 mm deep from the surface of the cortex). After the injection, the muscle and skin were sutured, and the wound was closed. A 3- to 4-week period was allowed for the Crh promoter-driven eGFP to be specifically expressed in the PVN-CRH neurons. Then, under deep anesthesia, the rats were perfused transcardially, and the brain was removed. The hypothalamic slices containing eGFP-tagged neurons were immunostained with a specific antibody against CRH. Colocalization of eGFP and CRH immunoreactivity validated that eGFP-tagged neurons expressed CRH. We then performed electrophysiological experiments in eGFP-tagged CRH-expressing neurons in hypothalamic slices. Because nonsecretory CRH-expressing neurons displayed a low threshold spike (LTS) whereas secretory CHR neurons did not, we first determined whether eGFP-tagged CRH displayed LTSs.

Intracerebroventricular (ICV) and PVN injections

For implanting an ICV cannula, rats under isoflurane anesthesia were placed on a stereotaxic instrument (David Kopf Instruments, Tujunga, CA). A 26-gauge guide cannula extending 3.5 mm from the pedestal (Plastics One, Roanoke, VA) was implanted through a 2-mm burr hole drilled in the skull 1.5 mm lateral to the midline and 1.0 mm caudal to the bregma. The guide cannula was affixed to the skull by using dental acrylic with 3 small machine screws. A dummy cannula extending 0.5 mm beyond the end of guide cannula was then inserted, and a dust cap was placed over the external end of the dummy cannula. After surgery,

buprenorphine (0.05 mg/kg) was injected subcutaneously for analgesia, and the rats were allowed to recover for 1 week. After a recovery period of a week, the dummy cannula was removed, and an injection cannula protruding 1.0 mm beyond the tip of the guide cannula was inserted into the guide cannula. Thus, the tip of the injection cannula targeted the lateral ventricle, which is 4.0-4.5 mm deep from the surface of the skull. The ICV injections were performed through the injection cannula connected to a Hamilton syringe. Each injection consisted of a 10-μl solution delivered over 1 minute. Bumetanide was dissolved in DMSO initially and then diluted in artificial cerebrospinal fluid (aCSF) (final concentration of DMSO was 0.5% v/v) at a concentration of 200 μM [33].

For the PVN injections, a bilateral guide cannula (26 gauge, 1.0 mm spacing between cannula, extending 7.0 mm from the pedestal; Plastics One) was implanted into the rat PVN. The tip of the guide cannula was positioned 1.0-mm dorsal to the intended drug injection site at the following coordinates (for PVN) according to Paxinos and Watson's atlas of the rat brain: 1.8 mm caudal and 0.5 mm lateral to the bregma and 8.0 mm ventral to the surface of the dura. As described for the guide cannula for ICV injection, the bilateral guide cannula for PVN injection was affixed to the skull by using dental acrylic, a dummy cannula was inserted into each side of the guide cannula, and a dust cap was then placed over the external end of the dummy cannula. After an 1-week recovery period the dummy cannula was removed and a bilateral injection cannula with tips protruding 1.0 mm beyond the tip of the guide cannula was placed. Gabazine (135 pmol in 100 nl of aCSF) was dissolved in aCSF and injected bilaterally into the PVN [46, 47]. Fluorescent microspheres (0.04 μm, wavelength 580 nm) in the same volume as gabazine were delivered through the cannula at the end of the experiment to mark the infusion sites.

Electrophysiological recordings in brain slices

Hypothalamic slices were prepared from the AAV-CRH-eGFP viral vector-injected rats. Briefly, the rats were decapitated under anesthesia with 2% isoflurane, and the brain was quickly removed and placed in ice-cold aCSF containing (in mM) 124.0 NaCl, 3.0 KCl, 1.3 $MgSO_4$, 2.4 $CaCl_2$, 1.4 NaH_2PO_4, 10.0 glucose, and 26.0 $NaHCO_3$ (continually gassed with a mixture of 95% O_2 and 5% CO_2). A tissue block containing the PVN was trimmed and fixed with tissue glue on the stage of a vibrating microtome (VT1000, Leica Biosystems Inc., Buffalo Grove, IL). Coronal slices 300 μm thick were cut as described previously [48-50]. Then, the slices were transferred to an incubation chamber containing aCSF continuously gassed with a mixture of 95% O_2 and 5% CO_2 at 34°C for at least 1 h before the electrophysiological recordings.

The slices in the recording chamber were perfused (3 ml/min) with aCSF (gassed with 95% O_2 and 5% CO_2) at a temperature of 34°C, which was maintained by using an in-line solution heater. We first identified eGFP-tagged neurons under an upright microscope (BX51WI; Olympus) equipped with epifluorescence illumination and differential interference contrast optics and performed cell-attached recordings in these neurons. The recording electrodes were pulled by using a micropipette puller (P-97; Sutter Instruments) from borosilicate capillaries (1.2 mm outer diameter, 0.68 mm inner diameter; World Precision Instruments). The resistance of the pipette was 3–6 MΩ when it was filled by an

internal solution containing (in mM) 140.0 K gluconate, 2.0 $MgCl_2$, 0.1 $CaCl_2$, 10.0 HEPES, 1.1 EGTA, 0.3 Na_2-GTP, and 2.0 Na_2-ATP, adjusted to pH 7.25 with 1 M KOH (270–290 mOsm). To record spontaneous firing activity, cell-attached recording was performed in eGFP-tagged neurons at a holding current of 0 pA. Electrical signals were processed by using a Multiclamp 700B amplifier (Molecular Devices), filtered at 1–2 kHz, and digitized at 20 kHz by using Digidata 1440 (Molecular Devices).

Cl^--impermeable gramicidin-perforated recordings were performed [33, 51] through a glass pipette containing an internal solution containing (in mM) 140 CsCl, 5 EGTA, and 10 HEPES, pH 7.4 adjusted with CsOH. Gramicidin was freshly dissolved in DMSO and then diluted into the pipette solution at a final concentration of 50 μg/ml. The tip of the recording pipette was back-filled with the internal pipette solution containing gramicidin. Also, the pipette solution contained a fluorescent dye, Lucifer yellow (0.5 mg/ml), to reveal whether the cell membrane was ruptured during recording. We determined E_{GABA} in PVN-CRH neurons on the basis of GABA currents elicited by puff application of GABA (100 μM) at a series of holding potentials ranging from −90 to −30 mV at 10-mV increments. The duration of GABA puff application was 15 ms to prevent the induction of HCO_3 currents by GABA [52]. CGP55845 (2 μM) and tetrodotoxin (1 μM) were added to the bath solution to block $GABA_B$ receptors and action potential-dependent synaptic activity, respectively. The access resistances of the perforated recording were between 40 to 70 MΩ.

Neurosecretory PVN neurons regulate HPA axis activity, whereas non-neurosecretory PVN-CRH neurons regulate autonomic system activity and display LTSs [53]. To determine whether the eGFP-tagged neurons displayed LTSs, a series of depolarizing current pulses (30–45 pA, 400 ms) from a membrane potential of −95 mV was applied to the recorded neuron. The eGFP-tagged PVN neurons showing no LTS were used for the recording experiments described below.

Quantification of NKCC1 and KCC2 protein levels in the PVN

Both NKCC1 and KCC2 protein levels in the PVN were determined by Western blotting in unstressed and CUMS rats. After the hypothalamic slices were sectioned, with the third ventricle used as a reference, the PVN tissue (~0.5 mm in diameter) spanning from 1.08 to 2.12 mm caudal to the bregma was micropunched bilaterally under a dissection microscope. Total protein was extracted by using the BCA method (Thermo Scientific) according to the manufacturer's instructions. The extracted protein samples were run in 4%-12% SDS-PAGE and transferred to polyvinylidene difluoride membrane (Immobilon P, Millipore). The immunoblots were probed with a rabbit anti-NKCC1 antibody (1:500, Abcam), rabbit anti-KCC2 antibody (1:500, Abcam), and rabbit anti-GAPDH (1:1000, ab37168, Abcam) for 24 h. On the second day, goat anti-rabbit HRP antibody (1:5000, Abcam) was applied to the immunoblots for 2 h at room temperature. An ECL kit (Life Sciences) was used to detect and enhance the protein bands, which were quantified by ImageJ software and normalized by the GAPDH optical density within the same samples.

Immunostaining for NKCC1 in PVN-CRH neurons

To determine the distribution of NKCC1 in the PVN-CRH neurons, we performed double fluorescence labeling by using antibodies against CRH and NKCC1. To enhance CRH immunoreactivity in the PVN, rats were injected intracerebroventricularly with 50–60 mg of colchicine [4]. Rats were deeply anesthetized (with sodium pentobarbital 50 mg/kg by intraperitoneal injection) and rapidly perfused transcardially with 0.9% saline followed by 4% paraformaldehyde in 0.1 M PBS (pH 7.4). The brains were removed and cut into 30-μm-thick frozen sections. After tissue sections were treated with blocking agent, they were incubated with the primary antibody mixture (for NKCC1: rabbit anti-NKCC1 antibody, Alphadiagnostic International (20); for CRH: guinea pig anti-CRF antibody, Peninsula Laboratories International, San Carlos, CA). The sections were incubated with a secondary antibody (for NKCC1, mouse anti-rabbit Alexa 488; for CRH, goat anti-guinea pig Alexa 594; Invitrogen, Carlsbad, CA). Confocal microscopy was used to visualize co-colocalization of the fluorescent markers.

Data analysis

Data were presented as means ± SEM. The junction potential was corrected based on different potentials by using internal and external solutions. The E_{GABA} was determined by using linear ¡regression to calculate a best-fit line for the voltage dependence of GABA-induced currents. The intercept of the current–voltage line with the abscissa (on the voltage axis) was taken as the E_{GABA}. For electrophysiological experiments, one neuron was recorded from one brain slice and at least 3 rats were included in each group. The Student t test was used to compare two datasets. For comparisons of more than two datasets, the repeated-measures ANOVA with Dunnett's post hoc test and two-way ANOVA with Bonferroni's post hoc test were performed to compare differences within and between groups, respectively. $P < 0.05$ was considered statistically significant.

Results

Identification of CRH-expressing neurons in the hypothalamus

PVN-CRH neurons play a pivotal role in regulation of the HPA axis and circulating CORT levels [54]. To reliably identify PVN-CRH neurons, we developed a novel AAV vector containing an eGFP gene under control of the rat CRH promoter (Fig. 1A). The AAV-CRH viral vector (1×10^{13} titer, 100 nl) was injected into the PVN. To determine whether this viral vector changed HPA activity, we measured circulating CORT levels 3 weeks after the injection. In 7 rats, the pre-injection circulating CORT levels did not significantly differ from CORT levels 3 weeks after injection of the AAV-CRH-eGFP vector ($P > 0.05$, Fig. 1B). Since AAV-CRH-eGFP vector did not change CORT levels. Thus, it was not necessary to test the effect of a control vector on circulating CORT levels. To validate that eGFP-tagged neurons were CRH-expressing neurons, we performed immunostaining by using specific antibody against CRH. The majority of eGFP-tagged (green) neurons (486 of 505 neurons, 96.2%) were CRH-immunopositive (red, Fig. 1C). With use of a fluorescent microscope, we directly identified these eGFP-tagged neurons in brain slices (Fig. 1D). Thus, we were able to perform electrophysiological recordings of these eGFP-tagged neurons. Because non-neurosecretory PVN neurons generate LTSs whereas neurosecretory PVN neurons do not

generate LTSs [53], we performed the electrophysiological experiments described below in eGFP-tagged neurons not displaying LTSs (Fig. 1E). We found that GFP-tagged neurons included both non-neurosecretory (with LTS) and neurosecretory (without LTS) neurons. The presence or absence of LTS were verified at either the beginning or the end of the recording.

Chronic stress impairs GABAergic inhibition in the PVN

Both 11-day and 20-day CUMS treatment significantly increased circulating CORT levels; the 11-day treatment (n = 8) increased levels from 13.1 ± 1.8 to 56.3 ± 3.1 ng/ml, and the 20-day treatment (n = 6) increased levels from 13.1 ± 1.8 to 59.7 ± 5.8 ng/ml ($P < 0.05$, Fig. 2A). Because the post-treatment circulating CORT levels did not differ between 11-day and 20-day CUMS treatment ($P > 0.05$, Fig. 2A), we used the 11-day CUMS treatment in the following experiments. Furthermore, sucrose preference was significantly decreased in the CUMS rats (n = 8) compared with that in 8 unstressed rats (Fig. 2B).

Since GABAergic inputs inhibit PVN neuroendocrine neurons to decrease circulating CORT levels [55], blockade of $GABA_A$ receptors in the PVN elicits a robust increase in corticosteroids [19, 55]. We thus determined whether synaptic GABAergic inhibition in the PVN is impaired in CUMS rats. Because bicuculline can excite neurons through its effect on small-conductance Ca^{2+}-activated K^+ channels in addition to blocking $GABA_A$ receptors [56], we chose another $GABA_A$ receptor antagonist, gabazine [57]. Microinfusion of gabazine (135 pmol in 100 nl of aCSF) through the implanted cannula into the PVN elicited a robust increase in circulating CORT levels in unstressed rats (Fig. 2C). In contrast, gabazine infusion had no effect on circulating CORT levels in CUMS rats (Fig. 2C). The microinfusion sites marked by fluorescent microspheres (0.04 μm) in the PVN were shown in Fig. 2D. This observation suggests that synaptic GABAergic inhibition in the PVN is markedly reduced in the chronic stress condition.

CUMS impairs GABA inhibition of PVN-CRH neurons and induces a depolarizing shift in E_{GABA}

Because $GABA_A$ receptor-mediated inhibition is dependent on intracellular Cl^- concentration, we assessed the alteration of GABAergic inhibition of eGFP-tagged PVN-CRH neurons by using cell-attached recording, which does not perturb intracellular Cl^-. The basal firing rate of eGFP-tagged PVN-CRH neurons was significantly higher in CUMS rats (1.8 ± 0.1 Hz, n = 7 neurons) than in unstressed rats (1.3 ± 0.1 Hz, n = 9 neurons, $P < 0.05$, Fig. 3). The PVN-CRH neurons displayed an irregular firing pattern without significant bursts, and this firing pattern of PVN-CRH neurons was not altered in CUMS rats. Bath application of the $GABA_A$ receptor antagonist gabazine (20 μM) [58, 59] significantly increased the firing rate of PVN-CRH neurons in unstressed rats (from 1.3 ± 0.1 to 2.0 ± 0.2 Hz, $P < 0.05$). In contrast, gabazine significantly decreased the firing rate in eGFP-tagged neurons in CUMS rats (from 1.8 ± 0.1 to 1.1 ± 0.1 Hz, $P < 0.05$, n = 9, Fig. 3A and B). Next, we determined the effect of the $GABA_A$ receptor agonist muscimol on the firing activity of PVN-CRH neurons. Bath application of muscimol (10 μM) significantly decreased the firing rate of PVN-CRH neurons in unstressed rats (from 1.4 ± 0.1 to 0.5 ± 0.1 Hz, $P < 0.05$, n = 8 neurons) but significantly increased the firing rate of PVN-CRH neurons in CUMS rats

(from 1.9 ± 0.1 to 3.0 ± 0.2 Hz, P< 0.05, n = 8 neurons, Fig. 3C and D). These observations suggest that $GABA_A$-mediated inhibition switched to excitation in PVN-CRH neurons after CUMS.

E_{GABA} is a key determinant of the neuronal response to activation of $GABA_A$ receptors, and a depolarizing shift in E_{GABA} leads to a switch from GABAergic inhibition to excitation in several pathological conditions [19, 33, 34]. Thus, we performed Cl^- impermeable gramicidin-perforated recordings in eGFP-tagged PVN-CRH neurons in hypothalamic slices to measure the E_{GABA} in unstressed and CUMS rats. The input resistances in eGFP-tagged neurons did not significantly differ between unstressed rats (1.3 ± 0.3 GΩ, n = 7 neurons) and CUMS rats (1.5 ± 0.4 GΩ, n = 8 neurons, P > 0.05). E_{GABA} in eGFP-tagged PVN neurons from CUMS rats (n = 8 neurons) displayed a significant depolarizing shift (about 20 mV) compared with E_{GABA} in eGFP-tagged PVN neurons from unstressed rats (n = 7 neurons, P < 0.05, Figure 4A-C). Bath application of $GABA_A$ receptor antagonist gabazine (20 μM) completely blocked GABA-induced currents (Figure 4D).

CUMS induces a long-lasting increase in NKCC1 protein levels and a transient reduction in KCC2 levels in the PVN

The Cl^- homeostasis of neurons in the central nervous system is primarily maintained by the Cl^- importing transporter NKCC1 and Cl^- extruding transporter KCC2 [18, 60, 61]. We determined the expression levels of NKCC1 and KCC2 by immunoblot analysis in PVN tissue obtained by the micropunch method in unstressed and CUMS rats. The 11-day CUMS treatment significantly increased NKCC1 protein band density by 94% ± 15% (n = 4 samples, P < 0.05) 3 days after completion of CUMS treatment and by 99% ± 25% (n = 4 samples, P < 0.05) 10 days after completion of CUMS treatment (Figure 5A and B). We performed 2-h restraint stress on unstressed rats in order to compare NKCC1 and KCC2 expression between acute stress and chronic stress. However, a 2-h acute restraint stress did not significantly increase NKCC1 protein levels (100% vs 123% ± 21%, n = 4 samples, P > 0.05, Fig. 5A). In another two groups of rats, the 20-day CUMS treatment significantly increased NKCC1 protein levels in the PVN by 92% ± 16% (n = 4 samples, P < 0.05, Figure 5E), which did not differ significantly from the increase in NKCC1 levels induced by 11-day CUMS treatment (86% ± 18%, n = 4 samples). NKCC1 levels were measured 5 days after completion of CUMS treatment. We also determined the NKCC1 expression on CRH-expressing neurons by performing immunohistochemical staining with antibodies against CRH and NKCC1. NKCC1 immunoreactivities were extensive in PVN-CRH neurons (Fig. 5F).

In addition, CUMS treatment significantly decreased the KCC2 protein level to 41% ± 9% (n = 4, P < 0.05) 3 days after completion of CUMS treatment. The KCC2 protein level returned to pre-CUMS levels within 5 days after completion of CUMS treatment (Figure 5C and D). In another 6 rats, 2-h restraint stress significantly decreased KCC2 protein level to 42 ± 12% (P > 0.05).

Increased NKCC1 activity contributes to the depolarizing shift in E_{GABA} and the resultant GABAergic excitation in PVN-CRH neurons in CUMS rats

It was previously reported that increased NKCC1 activity led to GABAergic excitation in neurons [33, 34, 62]. To determine whether upregulation of NKCC1 is involved in the switch from GABAergic inhibition to excitation, we assessed the effect of gabazine and muscimol on the firing activity of PVN-CRH neurons in brain slices treated with selective inhibitors of NKCC1. Incubating the brain slices with bumetanide (20 μM for 2–4 h) at a concentration that selectively inhibits NKCC1 [63] not only reduced the basal firing rate but also restored the stimulatory effects of gabazine on the firing activity of 8 PVN-CRH neurons from CUMS rats (Figure 6A and B). Furthermore, bumetanide-treatment restored the inhibitory effect of the $GABA_A$ receptor agonist muscimol the firing activity of PVN-CRH neurons from in CUMS rats (Figure 6C). In addition, bumetanide treatment (20 μM for 2–4 h) normalized the depolarizing shift in the E_{GABA} of PVN-CRH neurons in CUMS rats (Figure 6D and E). These findings indicate that increased NKCC1 activity contributes to the alteration of Cl^- homeostasis in PVN-CRH neurons in CUMS rats.

Inhibition of NKCC1 activity decreases circulating CORT levels in CUMS rats

Since inhibition of NKCC1 activity decreased the basal neuronal activity of PVN-CRH neurons and restored GABAergic inhibition in the PVN in CUMS rats, we determined the effect of NKCC1 inhibitor on circulating CORT levels in CUMS rats. CUMS treatment significantly increased basal CORT levels. Because the high-concentration (200 μM) bumetanide solution that is required for microinjection became viscous, which makes it difficult to administer microinjections into the PVN via a glass pipette with a small tip, we administered bumetanide through an ICV cannula. ICV administration of 200 μM bumetanide (10 μl) did not alter circulating CORT levels in unstressed rats (n = 8) but significantly decreased CORT levels (from 56.8 ± 3.9 to 24.5 ± 1.4 ng/ml) 30 min after bumetanide administration in CUMS rats (n = 6, Fig. 7). Within 2.5 h after ICV bumetanide injection, circulating CORT levels returned to the pre-injection level in CUMS rats.

Discussion

This study indicates that CUMS impairs GABAergic inhibition of PVN-CRH neurons through upregulation of NKCC1 in the PVN. We found that CUMS caused HPA axis hyperactivity and a profound depolarizing shift in E_{GABA} in PVN-CRH neurons. This depolarizing shift in E_{GABA} was associated with increased NKCC1 protein levels in the PVN. Inhibition of NKCC1 activity decreased PVN-CRH neuron activity and HPA axis activity by reestablishing GABAergic inhibition in the PVN. These findings reveal a novel mechanism that is responsible for impaired GABAergic inhibition in CUMS.

Previous studies have shown that chronic stress alters GABAergic inhibition in the amygdala [64], hippocampus [65], and PVN [36]. For example, chronic unpredictable stress decreases presynaptic GABAergic synaptic inputs and postsynaptic $GABA_A$ receptor expression levels in PVN neurons [36]. We found in this study that disinhibition of PVN neurons with the $GABA_A$ receptor antagonist gabazine increased circulating CORT levels. However, in CUMS rats, administration of gabazine in the PVN failed to change circulating CORT

levels. These data provide important *in vivo* evidence that the $GABA_A$-mediated inhibition of HPA axis activity and circulating CORT levels are markedly decreased under CUMS conditions. Since the PVN-CRH neurons are critical to the regulation of HPA axis activity and circulating CORT levels [3], we speculate that $GABA_A$-mediated inhibition of PVN-CRH neurons is altered after CUMS. To functionally assess the cellular mechanisms responsible for hyperactivity of PVN-CRH neurons, we identified these PVN-CRH neurons by specifically expressing eGFP under the control of CRH promoter. Our immunocytochemical staining revealed that most eGFP-tagged neurons were CRH-positive. Thus, this approach was able to distinguish PVN-CRH neurons in rat brain. This unique method of identifying PVN-CRH neurons in rat brain allowed us to assess neuronal function in our *in vitro* electrophysiological experiments.

Consistent with an increase in basal circulating CORT levels after CUMS, the basal firing activity of PVN-CRH neurons was significantly higher in CUMS rats than in unstressed rats. Strikingly, we found that $GABA_A$ receptor-mediated inhibition of PVN-CRH neurons switched to excitation in CUMS rats, as indicated by our finding that whereas gabazine increased the firing activity of PVN-CRH neurons in unstressed rats, gabazine induced an inhibitory effect on the firing activity of PVN-CRH neurons in CUMS rats. However, microinjection of gabazine into the PVN had no significant effect on circulating CORT level in CUMS rats. The reasons for these inconsistent effects of gabazine on the activity of PVN-CRH neurons in brain slice preparation and on circulating CORT levels *in vivo* are not clear. A previous study showed that chronic unpredictable stress leads to an increase in excitatory glutamatergic inputs to the PVN-CRH neurons [66]. It is possible that in *in vivo* conditions, gabazine-induced inhibition of PVN-CRH neurons was offset by enhanced excitatory glutamatergic inputs, which were severed in *in vitro* brain slice preparation.

Chronic unpredictable stress reduces the synaptic GABA release in the PVN and decreases $GABA_A$ receptor expression [35, 36]. However, the switch from $GABA_A$-mediated inhibition to excitation observed in this study could not be explained by the reduction in $GABA_A$ receptors or GABA release. It has been shown that a switch from GABA inhibition to excitation results from a depolarizing shift in E_{GABA} in several pathological conditions, including acute stress, early life stress, and chronic hyperosmotic stress [19, 21, 22]. We found that CUMS induced a depolarizing shift in E_{GABA} in PVN-CRH neurons compared with E_{GABA} in PVN-CRH neurons in unstressed rats. The depolarizing shift in E_{GABA} represents an increase in intracellular Cl^- concentration, which is determined by the cation-chloride co-transporters [17, 18]. Whereas KCC2 extrudes chloride, NKCC1 mediates chloride influx in neurons [17, 60]. Either KCC2 downregulation or NKCC1 upregulation leads to a depolarizing shift in E_{GABA} and a resultant switch from GABAergic inhibition to excitation [15, 17, 19, 21].

NKCC1 is expressed at a low level in the PVN in adult rats [67]. We found that the level of NKCC1 protein in the PVN was dynamically upregulated in response to CUMS treatment. It is not clear at what point NKCC1 protein levels in the PVN started to increase in response to CUMS. Our Western blot analysis revealed that NKCC1 protein levels were already increased 3 days after the completion of CUMS treatment. Furthermore, this increase in NKCC1 levels lasted for at least 10 days after the completion of CUMS treatment, whereas

acute restraint stress had little effect on NKCC1 levels. We also found that both acute restraint stress and CUMS led to decreased KCC2 protein levels in the PVN. However, KCC2 protein levels returned to basal levels seen in unstressed rats 5 days after completion of CUMS treatment. Therefore, it is likely that the observed depolarizing shift of E_{GABA} in the PVN-CRN neurons in CUMS was due to upregulation of NKCC1 but not to downregulation of KCC2. It seems that downregulation of KCC2 contributes to a depolarizing shift in E_{GABA} observed in acute stress and the early phase (up to 5 days) of the post-CUMS period, whereas upregulation of NKCC1 is the predominant contributor to the depolarizing shift in E_{GABA} in the late phase (after 5 days) of the post-CUMS period. It has been shown that chronic stress increases the response to new acute stressors [68]. The interaction between CUMS and 2-h restraint stress deserves future studies. The hypothalamic PVN is heterogeneous, containing several types of neurons, including PVN-CRH neurons; thus, the upregulation of NKCC1 in PVN tissue may not be due solely to an increase in NKCC1 level in PVN-CRH neurons in CUMS rats. Our immunohistochemical staining confirmed that NKCC1 immunoreactivity was present in the PVN-CRH neurons.

Since upregulation of NKCC1 is critical to the switch from GABAergic inhibition to excitation and to the depolarizing shift in E_{GABA} and in the PVN-CRH neurons, we conducted tests to determine whether inhibition of NKCC1 normalized the altered E_{GABA} and restored the excitatory effect of gabazine on PVN-CRH neurons in CUMS rats. Treatment of brain slices with the NKCC1 inhibitor bumetanide not only reduced the basal firing activity of PVN-CRH neurons in CUMS rats but also restored the excitatory effect of gabazine on the firing activity of PVN-CRH neurons in these rats. Furthermore, bumetanide treatment caused a hyperpolarizing shift in E_{GABA} in PVN-CRH neurons after CUMS. These data indicate that NKCC1 upregulation is a key mechanism contributing to the depolarizing shift in E_{GABA} and to the resultant inhibitory-to-excitatory switch in GABAergic control of PVN-CRH neurons in rats subjected to CUMS. It has been shown that acute exposure to a single stressor decreases KCC2 levels and results in a depolarizing shift in E_{GABA} in the PVN neurons [19]. The current study further found that prolonged exposure to multiple stressors leads to a depolarizing shift in E_{GABA}, which is due to an upregulation of NKCC1. Consistently, the important role of upregulation of NKCC1 in determining GABAergic excitation and the depolarizing shift of E_{GABA} has been observed previously in chronic hyperosmotic stress and spontaneously hypertensive rats [21, 33].

It has been shown that central administration of the NKCC1 inhibitor bumetanide reduces seizure progression [69] and sympathetic activity in neurogenic hypertension [33]. In this study, we found that inhibiting NKCC1 activity with bumetanide reduced circulating CORT levels in CUMS rats but did not change CORT levels in unstressed rats. Because the high-concentration bumetanide solution that is required for microinjection became viscous, which makes it difficult to perform microinjection into the PVN via a glass pipette with a small tip, we administered bumetanide through an ICV cannula to avoid injecting bumetanide directly into the PVN and thereby damaging PVN tissue. We realize that ICV-infused bumetanide can reduce NKCC1 activity in other brain regions, including the dorsal medial hypothalamus and anterior hypothalamus. Thus, the decreased circulating CORT levels in CUMS rats treated with bumetanide may result from inhibiting NKCC1 activity in multiple brain regions. Since the hypothalamic PVN is the main brain region that controls HPA axis

activity and circulating CORT levels, therefore, it is most likely that the PVN is the site mediating the effect of ICV bumetanide on circulating CORT levels. However, we cannot completely rule out the possibility that other brain regions are involved in the reduction in circulating CORT levels following ICV bumetanide infusion. The fact that NKCC1 upregulation induces a depolarizing shift in E_{GABA} and contributes to the increased excitability of PVN-CRH neurons indicates that NKCC1 is a potential target for developing effective therapeutics to reduce responsiveness of the HPA axis to chronic stress.

Acknowledgments

This study was supported by National Institute of Mental Health grant MH096086 and by an Institutional Research Grant from MD Anderson Cancer Center. This project was also supported by the National Cancer Institute under award number P30CA016672.

List of Abbreviations

AAV	adeno-associated virus
aCSF	artificial cerebrospinal fluid
E_{GABA}	GABA reversal potential
eGFP	enhanced green fluorescent protein
CORT	corticosterone
CRH	corticotrophin-releasing hormone
CUMS	chronic unpredictable mild stress
ICV	intracerebroventricular
HPA	hypothalamic-pituitary-adrenal
KCC2	K^+-Cl^--Cl^- cotransporter
LTS	low threshold spike
NKCC1	Na^+-K^+-Cl^--Cl^- cotransporter
PVN	paraventricular nucleus
PVN-CRH neurons	CRH-expressing neurons in the PVN
SpA	short synthetic polyadenylation
WPRE2	woodchuck post regulatory element 2

References

1. Krishnan V, Nestler EJ. The molecular neurobiology of depression. Nature. 2008; 455:894–902. [PubMed: 18923511]
2. Sapolsky RM. Why stress is bad for your brain. Science. 1996; 273:749–750. [PubMed: 8701325]

3. Ulrich-Lai YM, Herman JP. Neural regulation of endocrine and autonomic stress responses. Nat Rev Neurosci. 2009; 10:397–409. [PubMed: 19469025]

4. Bloom FE, Battenberg EL, Rivier J, Vale W. Corticotropin releasing factor (crf): Immunoreactive neurones and fibers in rat hypothalamus. Regul Pept. 1982; 4:43–48. [PubMed: 6750704]

5. Alon T, Zhou L, Perez CA, Garfield AS, Friedman JM, Heisler LK. Transgenic mice expressing green fluorescent protein under the control of the corticotropin-releasing hormone promoter. Endocrinology. 2009; 150:5626–5632. [PubMed: 19854866]

6. Wamsteeker Cusulin JI, Fuzesi T, Watts AG, Bains JS. Characterization of corticotropin-releasing hormone neurons in the paraventricular nucleus of the hypothalamus of crh-ires-cre mutant mice. PLoS One. 2013; 8:e64943. [PubMed: 23724107]

7. Itoi K, Talukder AH, Fuse T, Kaneko T, Ozawa R, Sato T, Sugaya T, Uchida K, Yamazaki M, Abe M, Natsume R, Sakimura K. Visualization of corticotropin-releasing factor neurons by fluorescent proteins in the mouse brain and characterization of labeled neurons in the paraventricular nucleus of the hypothalamus. Endocrinology. 2014; 155:4054–4060. [PubMed: 25057791]

8. Cullinan WE. Gaba(a) receptor subunit expression within hypophysiotropic crh neurons: A dual hybridization histochemical study. J Comp Neurol. 2000; 419:344–351. [PubMed: 10723009]

9. Decavel C, Van den Pol AN. Gaba: A dominant neurotransmitter in the hypothalamus. J Comp Neurol. 1990; 302:1019–1037. [PubMed: 2081813]

10. Herman JP, Mueller NK, Figueiredo H. Role of gaba and glutamate circuitry in hypothalamo-pituitary-adrenocortical stress integration. Ann N Y Acad Sci. 2004; 1018:35–45. [PubMed: 15240350]

11. Levy BH, Tasker JG. Synaptic regulation of the hypothalamic-pituitary-adrenal axis and its modulation by glucocorticoids and stress. Front Cell Neurosci. 2012; 6:24. [PubMed: 22593735]

12. Miklos IH, Kovacs KJ. Gabaergic innervation of corticotropin-releasing hormone (crh)-secreting parvocellular neurons and its plasticity as demonstrated by quantitative immunoelectron microscopy. Neuroscience. 2002; 113:581–592. [PubMed: 12150778]

13. Kaila K, Voipio J, Paalasmaa P, Pasternack M, Deisz RA. The role of bicarbonate in gabaa receptor-mediated ipsps of rat neocortical neurones. The Journal of physiology. 1993; 464:273–289. [PubMed: 8229801]

14. Bormann J, Hamill OP, Sakmann B. Mechanism of anion permeation through channels gated by glycine and gamma-aminobutyric acid in mouse cultured spinal neurones. The Journal of physiology. 1987; 385:243–286. [PubMed: 2443667]

15. Rivera C, Voipio J, Payne JA, Ruusuvuori E, Lahtinen H, Lamsa K, Pirvola U, Saarma M, Kaila K. The k+/cl− co-transporter kcc2 renders gaba hyperpolarizing during neuronal maturation. Nature. 1999; 397:251–255. [PubMed: 9930699]

16. Stein V, Hermans-Borgmeyer I, Jentsch TJ, Hubner CA. Expression of the kcl cotransporter kcc2 parallels neuronal maturation and the emergence of low intracellular chloride. J Comp Neurol. 2004; 468:57–64. [PubMed: 14648690]

17. Payne JA, Rivera C, Voipio J, Kaila K. Cation-chloride co-transporters in neuronal communication, development and trauma. Trends Neurosci. 2003; 26:199–206. [PubMed: 12689771]

18. Williams JR, Sharp JW, Kumari VG, Wilson M, Payne JA. The neuron-specific k-cl cotransporter, kcc2. Antibody development and initial characterization of the protein. J Biol Chem. 1999; 274:12656–12664. [PubMed: 10212246]

19. Hewitt SA, Wamsteeker JI, Kurz EU, Bains JS. Altered chloride homeostasis removes synaptic inhibitory constraint of the stress axis. Nat Neurosci. 2009; 12:438–443. [PubMed: 19252497]

20. Sarkar J, Wakefield S, MacKenzie G, Moss SJ, Maguire J. Neurosteroidogenesis is required for the physiological response to stress: Role of neurosteroid-sensitive gabaa receptors. J Neurosci. 2011; 31:18198–18210. [PubMed: 22171026]

21. Kim JS, Kim WB, Kim YB, Lee Y, Kim YS, Shen FY, Lee SW, Park D, Choi HJ, Hur J, Park JJ, Han HC, Colwell CS, Cho YW, Kim YI. Chronic hyperosmotic stress converts gabaergic inhibition into excitation in vasopressin and oxytocin neurons in the rat. J Neurosci; 2011; 31:13312–13322.

22. Gunn BG, Cunningham L, Cooper MA, Corteen NL, Seifi M, Swinny JD, Lambert JJ, Belelli D. Dysfunctional astrocytic and synaptic regulation of hypothalamic glutamatergic transmission in a

mouse model of early-life adversity: Relevance to neurosteroids and programming of the stress response. J Neurosci. 2013; 33:19534–19554. [PubMed: 24336719]

23. Yu J, Proddutur A, Elgammal FS, Ito T, Santhakumar V. Status epilepticus enhances tonic gaba currents and depolarizes gaba reversal potential in dentate fast-spiking basket cells. J Neurophysiol. 2013; 109:1746–1763. [PubMed: 23324316]
24. Lu Y, Zheng J, Xiong L, Zimmermann M, Yang J. Spinal cord injury-induced attenuation of gabaergic inhibition in spinal dorsal horn circuits is associated with down-regulation of the chloride transporter kcc2 in rat. The Journal of physiology. 2008; 586:5701–5715. [PubMed: 18845615]
25. Coull JA, Beggs S, Boudreau D, Boivin D, Tsuda M, Inoue K, Gravel C, Salter MW, De Koninck Y. Bdnf from microglia causes the shift in neuronal anion gradient underlying neuropathic pain. Nature. 2005; 438:1017–1021. [PubMed: 16355225]
26. Coull JA, Boudreau D, Bachand K, Prescott SA, Nault F, Sik A, De Koninck P, De Koninck Y. Trans-synaptic shift in anion gradient in spinal lamina i neurons as a mechanism of neuropathic pain. Nature. 2003; 424:938–942. [PubMed: 12931188]
27. Chen SR, Zhu L, Chen H, Wen L, Laumet G, Pan HL. Increased spinal cord na(+)-k(+)-2cl(-) cotransporter-1 (nkcc1) activity contributes to impairment of synaptic inhibition in paclitaxel-induced neuropathic pain. The Journal of biological chemistry. 2014; 289:31111–31120. [PubMed: 25253692]
28. Wake H, Watanabe M, Moorhouse AJ, Kanematsu T, Horibe S, Matsukawa N, Asai K, Ojika K, Hirata M, Nabekura J. Early changes in kcc2 phosphorylation in response to neuronal stress result in functional downregulation. J Neurosci. 2007; 27:1642–1650. [PubMed: 17301172]
29. van den Pol AN, Obrietan K, Chen G. Excitatory actions of gaba after neuronal trauma. J Neurosci. 1996; 16:4283–4292. [PubMed: 8753889]
30. Dzhala VI, Talos DM, Sdrulla DA, Brumback AC, Mathews GC, Benke TA, Delpire E, Jensen FE, Staley KJ. Nkcc1 transporter facilitates seizures in the developing brain. Nat Med. 2005; 11:1205–1213. [PubMed: 16227993]
31. Jin X, Huguenard JR, Prince DA. Impaired cl− extrusion in layer v pyramidal neurons of chronically injured epileptogenic neocortex. J Neurophysiol. 2005; 93:2117–2126. [PubMed: 15774713]
32. Pathak HR, Weissinger F, Terunuma M, Carlson GC, Hsu FC, Moss SJ, Coulter DA. Disrupted dentate granule cell chloride regulation enhances synaptic excitability during development of temporal lobe epilepsy. J Neurosci. 2007; 27:14012–14022. [PubMed: 18094240]
33. Ye ZY, Li DP, Byun HS, Li L, Pan HL. Nkcc1 upregulation disrupts chloride homeostasis in the hypothalamus and increases neuronal activity-sympathetic drive in hypertension. J Neurosci. 2012; 32:8560–8568. [PubMed: 22723696]
34. Kim YB, Kim YS, Kim WB, Shen FY, Lee SW, Chung HJ, Kim JS, Han HC, Colwell CS, Kim YI. Gabaergic excitation of vasopressin neurons: Possible mechanism underlying sodium-dependent hypertension. Circ Res. 2013; 113:1296–1307. [PubMed: 24103391]
35. Verkuyl JM, Karst H, Joels M. Gabaergic transmission in the rat paraventricular nucleus of the hypothalamus is suppressed by corticosterone and stress. Eur J Neurosci. 2005; 21:113–121. [PubMed: 15654848]
36. Verkuyl JM, Hemby SE, Joels M. Chronic stress attenuates gabaergic inhibition and alters gene expression of parvocellular neurons in rat hypothalamus. Eur J Neurosci. 2004; 20:1665–1673. [PubMed: 15355334]
37. Forbes NF, Stewart CA, Matthews K, Reid IC. Chronic mild stress and sucrose consumption: Validity as a model of depression. Physiol Behav. 1996; 60:1481–1484. [PubMed: 8946494]
38. Willner P, Towell A, Sampson D, Sophokleous S, Muscat R. Reduction of sucrose preference by chronic unpredictable mild stress, and its restoration by a tricyclic antidepressant. Psychopharmacology (Berl). 1987; 93:358–364. [PubMed: 3124165]
39. Haile CN, GrandPre T, Kosten TA. Chronic unpredictable stress, but not chronic predictable stress, enhances the sensitivity to the behavioral effects of cocaine in rats. Psychopharmacology (Berl). 2001; 154:213–220. [PubMed: 11314684]

40. Kosten TA, Galloway MP, Duman RS, Russell DS, D'Sa C. Repeated unpredictable stress and antidepressants differentially regulate expression of the bcl-2 family of apoptotic genes in rat cortical, hippocampal, and limbic brain structures. Neuropsychopharmacology. 2008; 33:1545–1558. [PubMed: 17700647]
41. Ortiz J, Fitzgerald LW, Lane S, Terwilliger R, Nestler EJ. Biochemical adaptations in the mesolimbic dopamine system in response to repeated stress. Neuropsychopharmacology. 1996; 14:443–452. [PubMed: 8726755]
42. D'Aquila PS, Newton J, Willner P. Diurnal variation in the effect of chronic mild stress on sucrose intake and preference. Physiol Behav. 1997; 62:421–426. [PubMed: 9251989]
43. Tonissaar M, Herm L, Rinken A, Harro J. Individual differences in sucrose intake and preference in the rat: Circadian variation and association with dopamine d2 receptor function in striatum and nucleus accumbens. Neurosci Lett. 2006; 403:119–124. [PubMed: 16682119]
44. Przybycien-Szymanska MM, Mott NN, Pak TR. Alcohol dysregulates corticotropin-releasing-hormone (crh) promoter activity by interfering with the negative glucocorticoid response element (ngre). PLoS One. 2011; 6:e26647. [PubMed: 22039522]
45. Hauck B, Chen L, Xiao W. Generation and characterization of chimeric recombinant aav vectors. Mol Ther. 2003; 7:419–425. [PubMed: 12668138]
46. Mandel DA, Schreihofer AM. Modulation of the sympathetic response to acute hypoxia by the caudal ventrolateral medulla in rats. J Physiol. 2009; 587:461–475. [PubMed: 19047207]
47. Tjen ALSC, Li P, Longhurst JC. Processing cardiovascular information in the vlpag during electroacupuncture in rats: Roles of endocannabinoids and gaba. J Appl Physiol (1985). 2009; 106:1793–1799. [PubMed: 19325030]
48. Li DP, Yang Q, Pan HM, Pan HL. Pre- and postsynaptic plasticity underlying augmented glutamatergic inputs to hypothalamic presympathetic neurons in spontaneously hypertensive rats. J Physiol. 2008; 586:1637–1647. [PubMed: 18238817]
49. Li DP, Byan HS, Pan HL. Switch to glutamate receptor 2-lacking ampa receptors increases neuronal excitability in hypothalamus and sympathetic drive in hypertension. J Neurosci. 2012; 32:372–380. [PubMed: 22219297]
50. Li DP, Chen SR, Pan HL. Angiotensin ii stimulates spinally projecting paraventricular neurons through presynaptic disinhibition. J Neurosci. 2003; 23:5041–5049. [PubMed: 12832527]
51. Ebihara S, Shirato K, Harata N, Akaike N. Gramicidin-perforated patch recording: Gaba response in mammalian neurones with intact intracellular chloride. J Physiol. 1995; 484(Pt 1):77–86. [PubMed: 7541464]
52. Grover LM, Lambert NA, Schwartzkroin PA, Teyler TJ. Role of hco3- ions in depolarizing gabaa receptor-mediated responses in pyramidal cells of rat hippocampus. J Neurophysiol. 1993; 69:1541–1555. [PubMed: 8389828]
53. Luther JA, Daftary SS, Boudaba C, Gould GC, Halmos KC, Tasker JG. Neurosecretory and non-neurosecretory parvocellular neurones of the hypothalamic paraventricular nucleus express distinct electrophysiological properties. J Neuroendocrinol. 2002; 14:929–932. [PubMed: 12472873]
54. Vale W, Spiess J, Rivier C, Rivier J. Characterization of a 41-residue ovine hypothalamic peptide that stimulates secretion of corticotropin and beta-endorphin. Science. 1981; 213:1394–1397. [PubMed: 6267699]
55. Cole RL, Sawchenko PE. Neurotransmitter regulation of cellular activation and neuropeptide gene expression in the paraventricular nucleus of the hypothalamus. J Neurosci. 2002; 22:959–969. [PubMed: 11826124]
56. Khawaled R, Bruening-Wright A, Adelman JP, Maylie J. Bicuculline block of small-conductance calcium-activated potassium channels. Pflugers Arch. 1999; 438:314–321. [PubMed: 10398861]
57. Hamann M, Desarmenien M, Desaulles E, Bader MF, Feltz P. Quantitative evaluation of the properties of a pyridazinyl gaba derivative (sr 95531) as a gabaa competitive antagonist. An electrophysiological approach. Brain Res. 1988; 442:287–296. [PubMed: 2453249]
58. Heaulme M, Chambon JP, Leyris R, Wermuth CG, Biziere K. Characterization of the binding of [3h]sr 95531, a gabaa antagonist, to rat brain membranes. J Neurochem. 1987; 48:1677–1686. [PubMed: 3033146]

59. Park JB, Skalska S, Son S, Stern JE. Dual gabaa receptor-mediated inhibition in rat presympathetic paraventricular nucleus neurons. J Physiol. 2007; 582:539–551. [PubMed: 17495040]

60. Kahle KT, Staley KJ, Nahed BV, Gamba G, Hebert SC, Lifton RP, Mount DB. Roles of the cation-chloride cotransporters in neurological disease. Nat Clin Pract Neurol. 2008; 4:490–503. [PubMed: 18769373]

61. Mercado A, Mount DB, Gamba G. Electroneutral cation-chloride cotransporters in the central nervous system. Neurochem Res. 2004; 29:17–25. [PubMed: 14992262]

62. Choi HJ, Lee CJ, Schroeder A, Kim YS, Jung SH, Kim JS, Kim do Y, Son EJ, Han HC, Hong SK, Colwell CS, Kim YI. Excitatory actions of gaba in the suprachiasmatic nucleus. J Neurosci. 2008; 28:5450–5459. [PubMed: 18495878]

63. Delpy A, Allain AE, Meyrand P, Branchereau P. Nkcc1 cotransporter inactivation underlies embryonic development of chloride-mediated inhibition in mouse spinal motoneuron. J Physiol. 2008; 586:1059–1075. [PubMed: 18096599]

64. Liu ZP, Song C, Wang M, He Y, Xu XB, Pan HQ, Chen WB, Peng WJ, Pan BX. Chronic stress impairs gabaergic control of amygdala through suppressing the tonic gabaa receptor currents. Mol Brain. 2014; 7:32. [PubMed: 24758222]

65. MacKenzie G, Maguire J. Chronic stress shifts the gaba reversal potential in the hippocampus and increases seizure susceptibility. Epilepsy research. 2015; 109:13–27. [PubMed: 25524838]

66. Ziegler DR, Cullinan WE, Herman JP. Organization and regulation of paraventricular nucleus glutamate signaling systems: N-methyl-d-aspartate receptors. The Journal of comparative neurology. 2005; 484:43–56. [PubMed: 15717303]

67. Kanaka C, Ohno K, Okabe A, Kuriyama K, Itoh T, Fukuda A, Sato K. The differential expression patterns of messenger rnas encoding k-cl cotransporters (kcc1,2) and na-k-2cl cotransporter (nkcc1) in the rat nervous system. Neuroscience. 2001; 104:933–946. [PubMed: 11457581]

68. Marti O, Gavalda A, Gomez F, Armario A. Direct evidence for chronic stress-induced facilitation of the adrenocorticotropin response to a novel acute stressor. Neuroendocrinology. 1994; 60:1–7.

69. Sivakumaran S, Maguire J. Bumetanide reduces seizure progression and the development of pharmacoresistant status epilepticus. Epilepsia. 2015

Key points summary

- Chronic stress diminished GABA inhibition in the PVN and induced a depolarizing shift in E_{GABA} in CRH-expressing PVN neurons.
- Upregulation of NKCC1 in the PVN contributed to the depolarizing shift in E_{GABA} and the resultant GABAergic excitation in chronic stress.
- Inhibition of NKCC1 activity decreased circulating corticosterone levels in chronic stress.

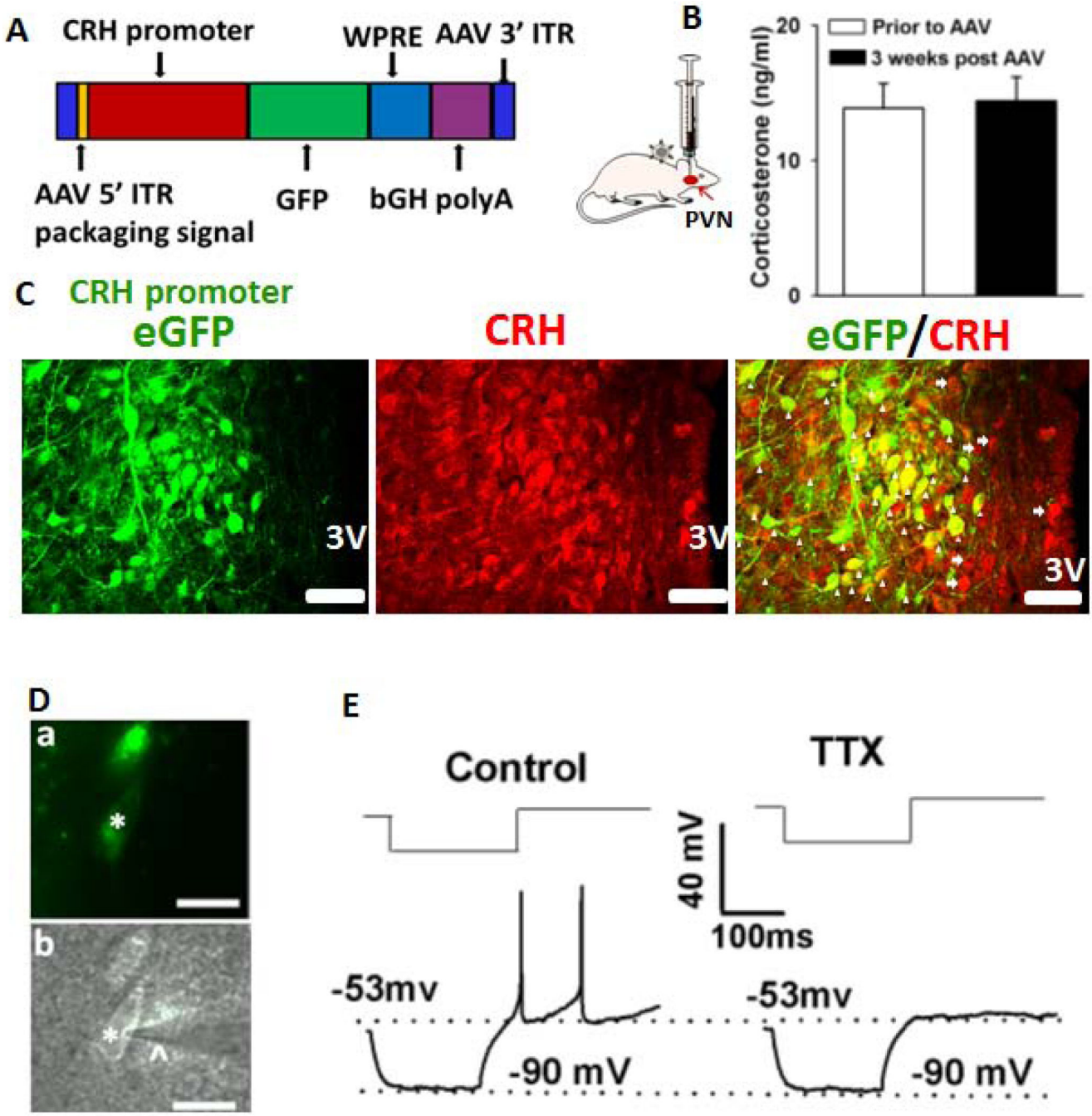

Figure 1. Identification of PVN-CRH neurons

(A): Construct of AAV vector containing an eGFP gene under control of the rat CRH promoter. (B): Summary data show no significant change in circulating CORT levels prior to and 3 weeks after AAV-CRH vector injection (n = 7 rats, P > 0.05, paired *t* test). (C): Immunostaining depicts eGFP-tagged neurons as CRH immunopositive. The arrowheads indicate neurons with both eGFP and CRH immunoreactivity. The arrows indicate CRH-positive neurons without eGFP immunoreactivity. 3V, third ventricle. (D): eGFP-tagged PVN neurons (*) with an attached recording electrode (^) viewed with fluorescence

illumination (a) and infrared differential interference contrast optics (b) in the brain slice. (E): Electrophysiological recordings showed that an eGFP-tagged neuron did not generate LTSs in response to depolarizing current pulses (30–45 pA) from a membrane potential of −90 mV in the absence and presence of 1 μM tetrodotoxin (TTX). Scale bars indicate 50 μm in C and 20 μm in D.

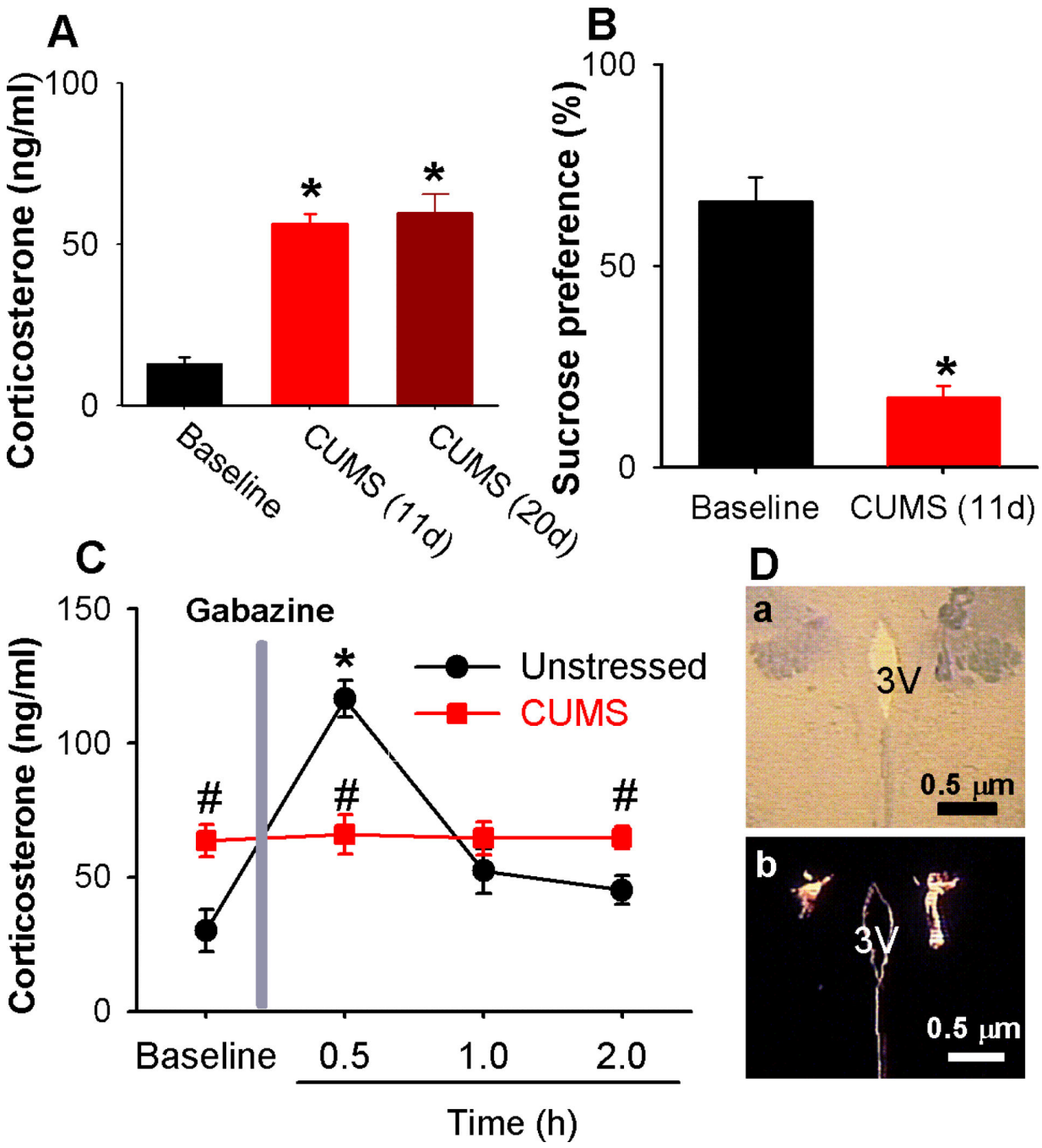

Figure 2. CUMS impairs $GABA_A$-mediated inhibition in the PVN

(A): Both 11-day CUMS treatment and 20-day CUMS treatment significantly increased circulating CORT levels. (n = 8 rats for 11-day CUMS and n = 6 rats for 20-day CUMS, $P < 0.05$, repeated-measures ANOVA with Dunnett's post hoc test). (B): CUMS significantly suppressed sucrose preference (n = 8 rats in each group, $P < 0.05$, paired *t* test). (C): Change in circulating CORT levels after microinjection of the $GABA_A$ antagonist gabazine into the PVN (n = 6 rats in each group, * $P < 0.05$ compared with the basal value, repeated-measures ANOVA with Dunnett's post hoc test, # $P < 0.05$ compared with values in unstressed group,

unpaired *t* test). (D): Photomicrographic images depict the microinfusion sites marked by fluorescent microspheres (0.04 μm, wavelength 580 nm) in the PVN in light optics (a) and fluorescent illumination (b). 3V, third ventricle. All data are expressed as mean ± s.e.m.

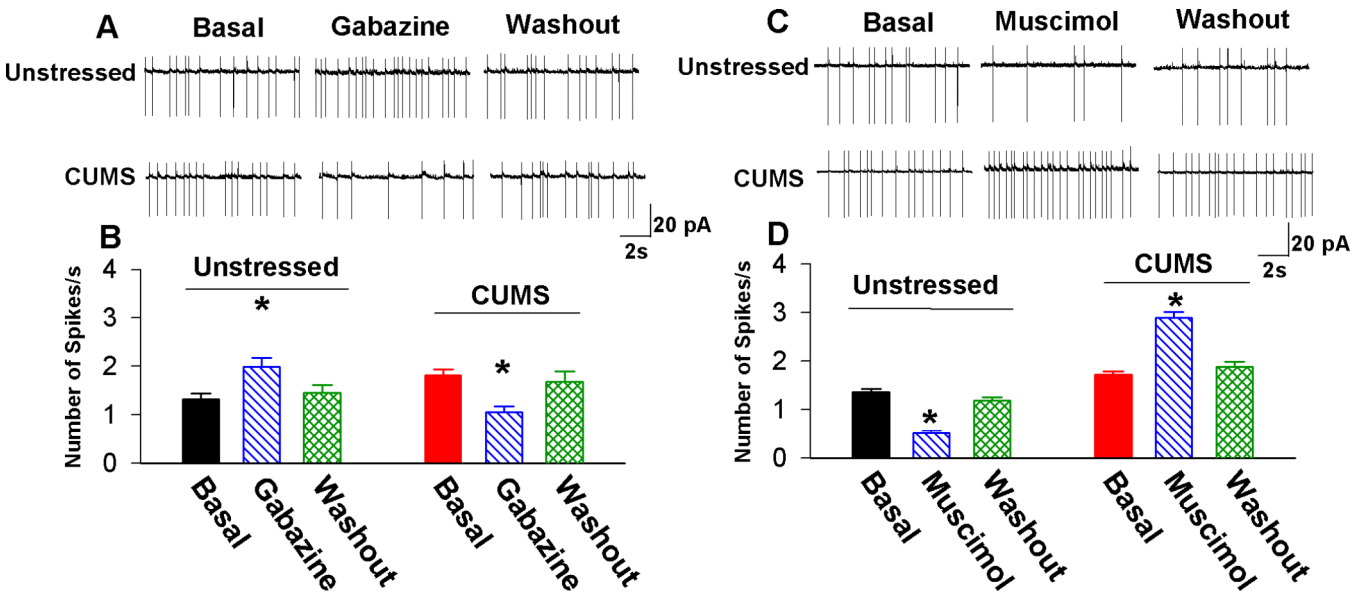

Figure 3. GABAergic inhibition of PVN-CRH neurons is diminished in CUMS rats

(A, B): Original recordings (A) and summary data (B) show that blocking $GABA_A$ receptors with gabazine (20 μM) significantly increased firing activity of eGFP-tagged PVN neurons in unstressed rats but decreased firing activity of PVN neurons in CUMS rats (n = 9 neurons in unstressed rats and n = 9 neurons in CUMS rats; * $P < 0.05$ compared with the basal value of each group, repeated-measures ANOVA with Dunnett's post hoc test). (C, D): Original recordings (C) and summary data (D) show that stimulation of $GABA_A$ receptors with muscimol (10 μM) significantly decreased firing activity of eGFP-tagged PVN neurons in unstressed rats but increased firing activity of PVN neurons in CUMS rats (n = 8 neurons in unstressed rats and n = 8 neurons in CUMS rats; * $P < 0.05$ compared with the basal value of each group, repeated-measures ANOVA with Dunnett's post hoc test).

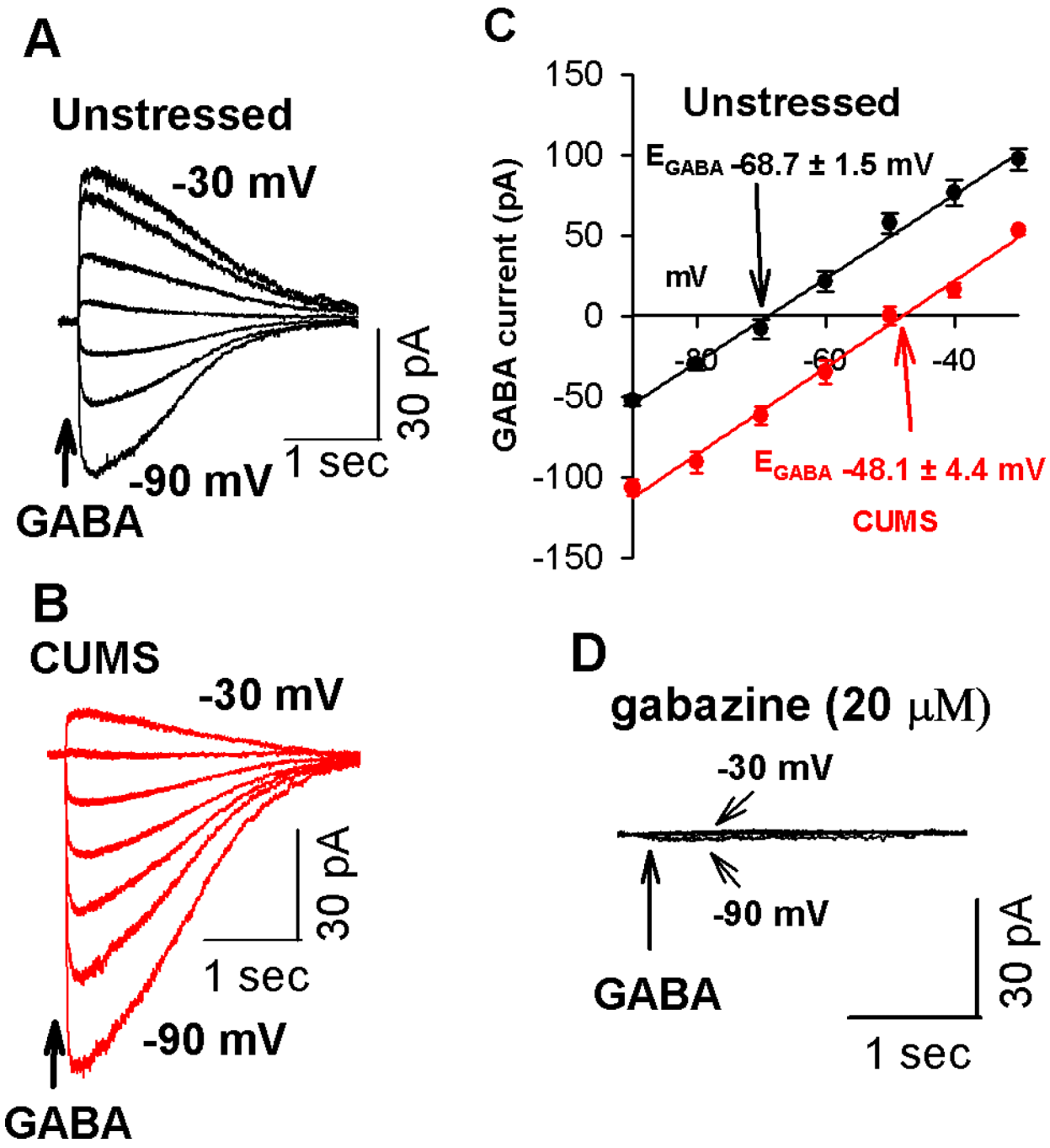

Figure 4. CUMS induces a depolarizing shift of the E_{GABA} in PVN-CRH neurons

(A, B): Original traces show gramicidin-perforated recordings of GABA-induced currents at a series of membrane potentials from −90 to −30 mV of PVN-CRH neurons from 1 unstressed rat (A) and 1 CUMS rat (B). (C): Mean changes in the E_{GABA} in the PVN-CRH neurons in unstressed (n = 7 neurons) and CUMS rats (n = 8 neurons). Note that the E_{GABA} underwent a depolarizing shift in CUMS rats but not in unstressed rats. (D): Raw recordings show that GABA-induced currents were completely blocked by $GABA_A$ receptor antagonist gabazine (20 μM) in an eGFP-tagged PVN neuron from an unstressed rat.

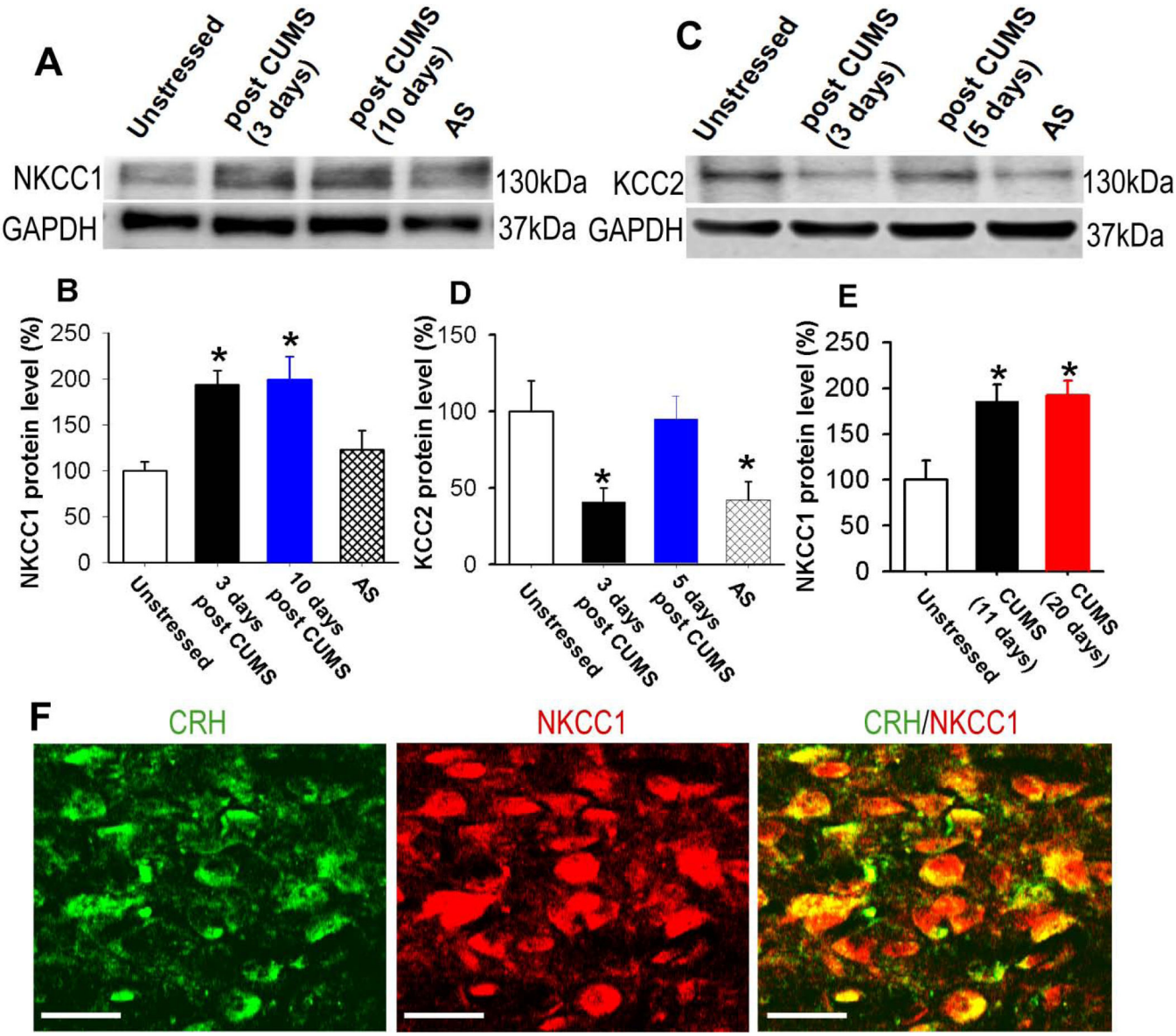

Figure 5. Chronic stress upregulates NKCC1 in the PVN

(A and B): Immunoblots (A) and quantification (B) of NKCC1 protein levels in the PVN tissue in unstressed, 3 days and 10 days after completion of CUMS treatment, and 2-h acute restraint stress (AS) rats (n = 4 samples in each group). The molecular weight is indicated to the right of the gel images. C and D: Immunoblots (C) and quantification (D) of KCC2 protein levels in the PVN in unstressed rats and 3 days and 10 days after completion of CUMS treatment, and 2-h acute restraint stress (AS) rats (n = 4 samples in each group). The molecular weight is indicated to the right of the gel images. (E): NKCC1 expression levels in the PVN in unstressed, 11-day CUMS, and 20-day CUMS rats. NKCC1 levels were measured 5 days after completion of CUMS treatment. (F): Confocal images depicting the presence of NKCC1 (red) on CRH-expressing neurons (green). All images are single confocal optical sections. Scale bars indicate 20 μm. * $P < 0.05$ compared with the value in

unstressed rats, repeated-measures ANOVA with Dunnett's post hoc test. AS: 2-h acute restraint stress.

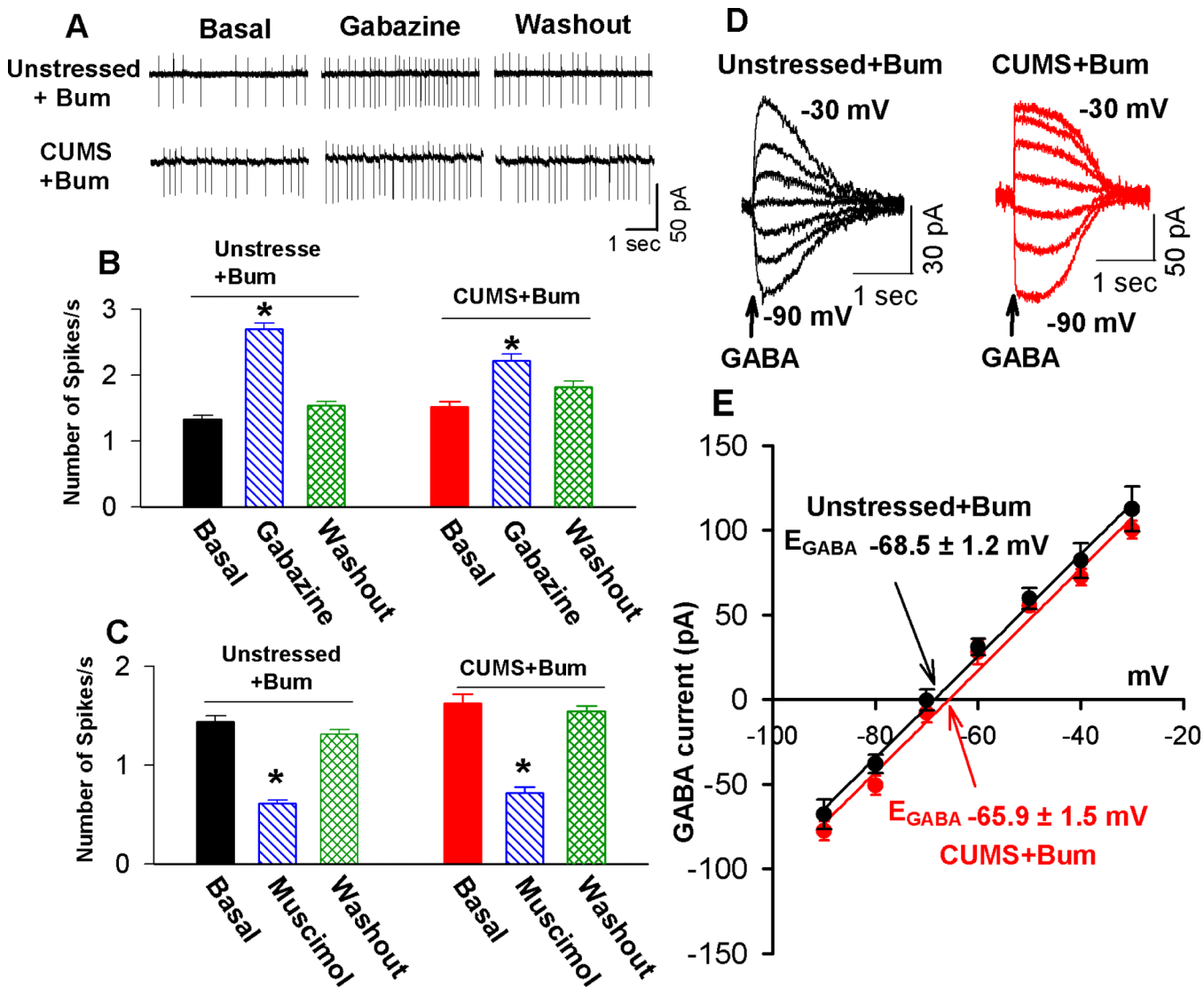

Figure 6. Inhibition of NKCC1 normalizes GABA inhibition and the E_{GABA} of PVN-CRH in CUMS rats

(A, B): Original traces (A) and summary data (B) show the effect of gabazine on the firing activity in PVN-CRH neurons in slices treated with bumetanide in unstressed and CUMS rats (n = 7 neurons in unstressed rats and n = 8 neurons in CUMS rats; * $P < 0.05$ compared with the basal value of each group, repeated-measures ANOVA with Dunnett's post hoc test). (C): Summary data show the effect of muscimol on the firing activity of PVN-CRH neurons in slices treated with bumetanide in unstressed and CUMS rats (n = 7 neurons in unstressed rats and n = 7 neurons in CUMS rats; * $P < 0.05$ compared with the basal value of each group, repeated-measures ANOVA with Dunnett's post hoc test). (D, E): Original recordings (D) and summary data (E) show GABA currents recorded at various holding potentials and the E_{GABA} of eGFP-tagged PVN neurons in brain slices treated with vehicle (n = 7 neurons) and bumetanide (n = 6 neurons) in unstressed and CUMS rats.

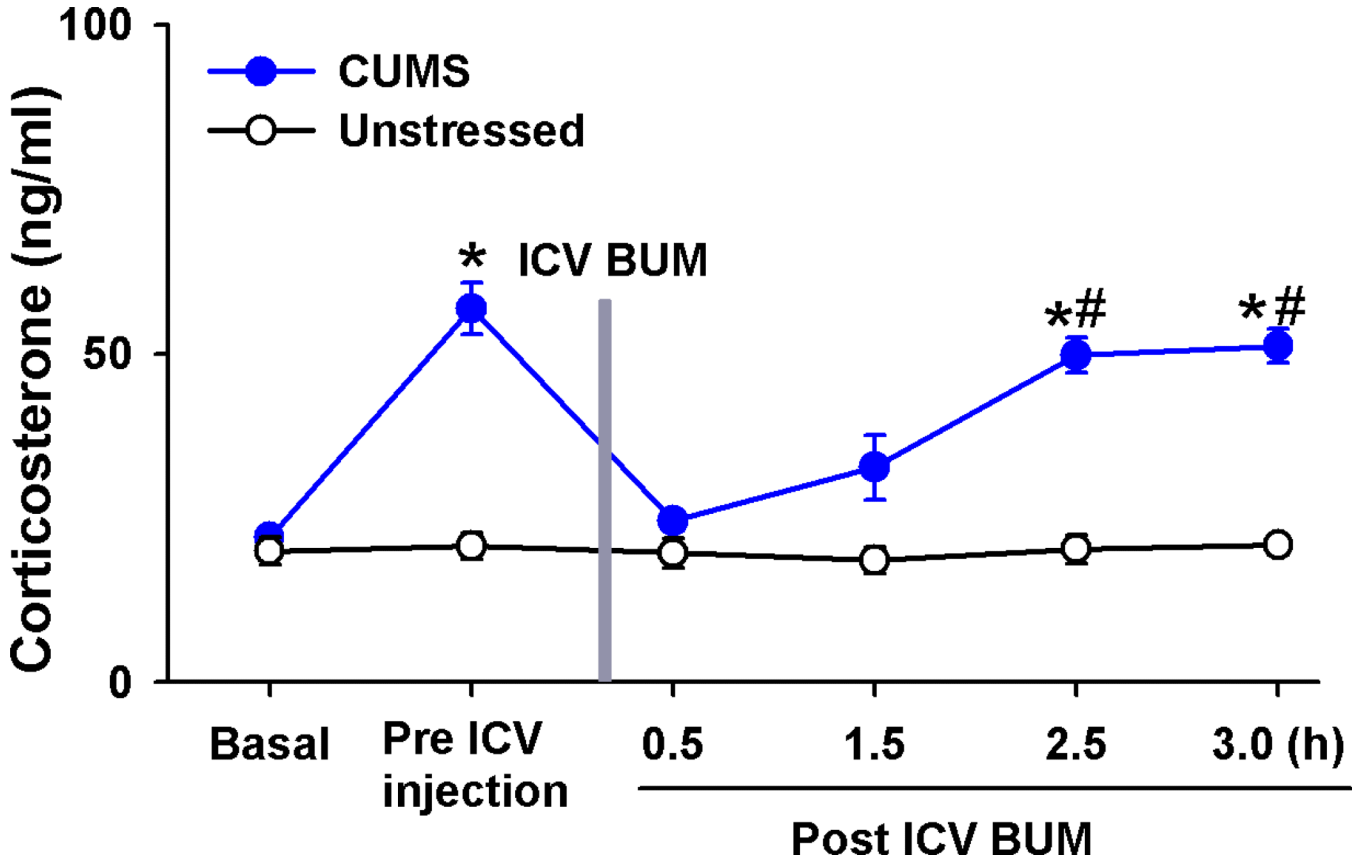

Figure 7. Inhibition of central NKCC1 activity normalizes circulating CORT levels in CUMS rats

Summary data show circulating CORT levels during basal condition, pre and post ICV administration of bumetanide in unstressed rats (n = 7) and CUMS rats (n = 8). * $P < 0.05$ compared with the basal value, repeated-measures ANOVA with Dunnett's post hoc test, # $P < 0.05$ compared with values in unstressed group, unpaired *t* test).